# Impact of the processing temperature on the crystallization behavior and mechanical properties of poly[R-3-hydroxybutyrate-co-(R-3-hydroxyvalerate)]

Julie Bossu, Nicolas Le Moigne, Philippe Dieudonne-George, Loïc Dumazert, Valérie Guillard, Helene Angellier-Coussy

# Impact of the processing temperature on the crystallization behavior and mechanical properties of poly[R-3-hydroxybutyrate-co-(R-3-hydroxyvalerate)]

Julie Bossu[1*], Nicolas Le Moigne[2], Philippe Dieudonné-George[3], Loïc Dumazert[2], Valérie Guillard[1], Hélène Angellier-Coussy[1*]

[1] *IATE, Univ Montpellier, INRAE, Institut Agro, Montpellier, France*

[2] *Polymers Composites and Hybrids (PCH), IMT Mines Ales, Ales, France*

[3] *Laboratoire Charles Coulomb (L2C), Univ. Montpellier, CNRS, Montpellier, France*

* juliebossu@hotmail.fr

* helene.coussy@umontpellier.fr

## HIGHLIGHTS

- The crystalline structure of PHBV is strongly impacted by processing temperature;
- Above a critical temperature, a segregation occurs between PHB-rich and PHV-rich domains;
- Thermo-regulated WAXS experiments show a great interest in studying PHBVs' melting and crystallization;
- NMR analysis confirmed the existence of irreversible changes in macromolecular structure with temperature;
- Mechanical tests are critical to define a suitable processing window.

## ABSTRACT

Poly[R-3-hydroxybutyrate-co-(R-3-hydroxyvalerate)] (PHBVs) are promising biopolymers, which could substitute petro-based plastics for packaging applications. To anticipate the behavior of PHBVs when transformed using conventional thermo-mechanical shaping processes, it is needed to better understand the effect of processing temperature on their crystallization behavior and final properties. The objectives of the present work were thus (1) to better understand the influence of the processing temperature on the PHBV macromolecular and crystalline structures, depending on its HV content, and (2) to define a processing window guaranteeing optimized mechanical properties of PHBV films. An innovative experimental strategy was proposed, enabling the study of melting and crystallization events, crystalline structure changes, and evolution of mechanical properties of PHBV according to processing temperature, using identical thermal cycles. A comprehensive dynamic monitoring of the studied PHBVs was achieved by coupling differential scanning calorimetry (DSC), thermogravimetric analysis (TGA), step scan DSC (SDSC), observations of isothermal crystallization under polarized optical microscopy (POM), thermo-regulated wide angle X-ray analysis (WAXS), Nuclear Magnetic Resonance (NRM), and finally mechanical tests on PHBV films. The combination of these experiments revealed how inappropriate processing temperatures can result in irreversible changes in PHBVs' macromolecular and crystalline structures, thermal behavior and mechanical performances. When increasing the HV content of the copolymer, adjusting the processing conditions according to these results revealed to be critical to match the functional properties targeted for a specific use.

## KEYWORDS

Biodegradable copolymer; 3-hydroxyvalerate content; thermal degradation; crystallization; phase segregation; process optimization

## INTRODUCTION

Polyhydroxyalkanoates (PHA's) are bacterial polyesters that are fully biodegradable in natural conditions and can be produced from renewable sources, including organic wastes, by a variety of microorganisms [1–3]. Among PHA's, the most commonly investigated and easiest to produce is the homopolymer poly-3-hydroxybutyrate (PHB). However, its high crystallinity and glass transition temperature result in fairly stiff and brittle materials [4], limiting its use as a general-purpose plastic substitute (i.e. elongation at break is about 2% compared to up to 400% for some polyolefins). An approach to address this problem is the incorporation of 3-hydroxyvalerate units (HV units) in the molecular structure of PHB to produce poly[R-3-hydroxybutyrate-co-(R-3-hydroxyvalerate)] copolymers (PHBV). Indeed, the resulting decrease of overall crystallinity and glass transition temperature is likely to lead to a better processability and a significant improvement of the material ductility [5].

PHBV-based materials display contrasting functional properties depending on their macromolecular and crystalline structures, which are strongly related to their HV content, the comonomer compositional distribution, the molar mass and the sample purity [6,7]. The macromolecular and crystalline structures can also be strongly affected by the processing conditions such as melting and cooling temperatures and rates [8]. As a consequence, even if the synthesis and macromolecular structure of PHBV have been optimized (i.e. increased HV content), its final functional properties can be limited due to inadequate processing conditions. Defining optimal processing conditions that would allow maximizing the copolymer's final technical performance thus appears as a critical and necessary step for their implementation in general-purpose plastic applications. In particular, the impact of HV content on the thermal sensitivity towards processing conditions is still unclear and thus deserves more consideration. Surprisingly, while the influence of the cooling/heating rate and the holding time in the melt on the overall crystallinity and final mechanical properties has already been studied for PHB [8], this subject is not documented for PHBV copolymers with varying HV contents.

The main difficulty in studying the impact of thermal treatment on the crystalline structure of PHBV products relies on the complexity of interpreting their thermograms, showing multiple melting peaks in the case of high HV contents [1]. This makes difficult to understand the effective changes that occur within their crystalline structure. The occurrence of multiple melting peaks generally reflects the presence of varying microstructures, i.e. different nature of sizes of crystals. Gunaratne and Shanks [1] reported that, for a HV content ranging from 8 to 12 %, the first melting endotherm corresponded to the melting of crystals formed with low thermal stability through isothermal crystallization, and that the second melting endotherm was due to the melting of stable crystals formed through reorganization during the second heating scan. Another analysis of multiple melting behavior in PHBV materials is that it could also result from a melting-recrystallization phenomenon during DSC heating process [25]. Considering this melting-recrystallization phenomenon, the low-temperature and high-temperature melting peaks are attributed to the prior melting of a part of the original crystals and the subsequent melting of crystals formed through the melt-recrystallization process during the heating scan, respectively [26].

Different authors reported that a variation of energy in the system could modify the degree of incompatibility between the different blocks of semi-crystalline copolymers, leading to different microstructural organizations upon crystallization [27–29]. Since PHBV copolymers are composed of HB and HV units, a similar mechanism is likely to occur. Laycock already proposed that HB-rich domains and HV-rich domains could be more or less miscible [30]. Thus, the existence of double melting peaks could be reasonably attributed to the melting of PHB-rich and PHV-rich crystal populations.

For this reason, the processing conditions used to transform PHBV raw powders into films must be carefully chosen. The temperature of the melt and the holding time of the polymer in the melt are usually fixed to erase previous thermal history, so that all traces of existing crystal nuclei are destroyed. If the melting temperature or holding time in the melt are too low, the remaining partially ordered crystalline regions can act as predetermined athermal nucleation sites, inducing self-nucleation and resulting in earlier crystallization. On the other hand, an excessive melting to erase thermal and crystallization history can induce thermal degradation, and thus a decrease of molar mass [9], which in turn affects the crystallization rate, crystalline structure and properties of the final product. In this regard, a suitable processing temperature threshold needs to be found to enable satisfying melting of the crystals while avoiding thermal degradation. In addition, HB and HV units' interactions within PHBV's structure have been proved to be critical for the material final properties [7]. For this reason, particular attention must be paid to the effect of processing temperature on the co-crystallization of dissimilar domains constituting the copolymer.

In this context, the objectives of the present study are (1) to better understand the influence of the processing temperature on the PHBV macromolecular and crystalline structures, depending on its HV content, and (2) to define a processing window guarantying optimized mechanical properties of PHBV films. For that purpose, an innovative experimental strategy is proposed in this work, enabling to study melting and crystallization events, crystalline structure changes, and evolution of mechanical properties of PHBV along temperature, using identical thermal cycles. A comprehensive dynamic monitoring of two PHBV copolymers, having contrasted macromolecular structures (i.e. 1-3 % and 18 % HV contents, the first one produced from pure culture and the second one produced from mixed culture), is achieved by coupling differential scanning calorimetry (DSC), step scan DSC (SDSC), observations of isothermal crystallization under polarized optical microscopy (POM), thermo-regulated wide angle X-ray analysis (WAXS), Nuclear Magnetic Resonance (NRM), and finally mechanical tests on thin PHBV films.

## EXPERIMENTAL

### Materials

PHBV with 18 mol% of 3-hydroxyvalerate units (HV) (denoted as PHBV18%) of high purity (98.6% according to Inductively Coupled Plasma - Atomic Emission Spectroscopy) in the form of pure uncompounded powder was obtained from the Institute of Experimental and Technological Biology (iBET, Lisbon, Portugal), where it was prepared from apple fruit pulp and waste waters as described in Bossu et al. (2020). Gel permeation chromatography was used to obtain the number-average molar mass (Mn), weight-average molar mass (Mw) and polydispersity index ($I_P$=Mw/Mn). The obtained results for PHBV18% were respectively Mn = 94 411 g.mol$^{-1}$, Mw = 366 000 g.mol$^{-1}$ and $I_P$ = 3.88. PHBV with 3 mol% of 3-hydroxyvalerate units (HV) (denoted as PHBV3%) was purchased from Natureplast (France). It corresponds to the PHI003 commercial grade, a pure uncompounded powder produced from pure culture (Mn = 520 001 g.mol$^{-1}$, Mw = 1 124 507 g.mol$^{-1}$ and $I_P$ = 2.16). In a previous work, it has been reported that PHBV18% is a block-copolymer with macromolecular chains consisting in successive PHB and PHV blocks characterized by different crystallization behaviors [7].

### Differential scanning calorimetry (DSC)

DSC analyses were carried out using a TA Instruments (Q200 modulated DSC, TA Instruments, New Castle, USA) calorimeter under a nitrogen atmosphere with a flow rate of 50 mL.min$^{-1}$ and at a heating rate of 10 °C.min$^{-1}$. Around 12 mg of sample was used for each analysis and all experiments were done in duplicate.

The key parameters obtained by DSC in a previous work [7] for PHBV3% and PHBV18%, based on heating (up to 180°C) and cooling (down to -30°C) scans at 10 °C.min$^{-1}$ and under a nitrogen flow, are given in Table 1.

**Table 1.** Key DSC parameters ($Tm_0$: first melting temperature; $\Delta H_0$: corresponding melting enthalpy; $Xc_0$: degree of crystallinity calculated from ΔH0) and key WAXS parameters (lattice parameters a, b and c; calculated from planes (110), (020) for a and b respectively, and from the mean value obtained from planes (101), (021) and (121) for c) calculated for the studied polymers from previous characterization [7]. Numbers in brackets indicate standard deviations values.

| | DSC | | | WAXS | | |
|---|---|---|---|---|---|---|
| | $Tm_0$ (°C) | $\Delta H_0$ (J/g) | $Xc_0$ (%) | a (nm) | b (nm) | c (nm) |
| PHBV 3% | 174.3 (0.21) | 100.6 (5.2) | 68.9 (3.6) | 0.566 | ~~1.303~~ 1.300 | ~~0.588~~ 0.5899 |
| PHBV 18% | 138.5 (0.08) | 76.3 (3.3) | 52.3 (2.2) | ~~0.572~~ 0.570 | ~~1.314~~ 1.307 | ~~0.686~~ 0.5904 |

In the present work, non-isothermal crystallization of PHBV3% and PHBV18% was monitored after a first isothermal various preheating temperatures (*Tph*) to analyze the effect of preheating temperature on the crystallization process. For that purpose, PHBV powder samples were first heated until *Tph* (first heating scan) and stabilized for 3 min; then cooled down until -30 °C (cooling scan) and stabilized for 3 min; and finally heated again until 190 °C (second heating scan). Heating and cooling rates were set to 10 °C.min$^{-1}$. The melting temperatures ($Tm_1$ in case of a single melting endotherm; $Tm_1$ and $Tm_2$ in case of double melting endotherm), the glass transition temperature (*Tg*), the melt crystallization temperature (*Tc)* and the cold crystallization temperature (*Tcc*) were determined from the obtained DSC curves. Melting enthalpies were calculated by integrating the endothermic peaks, normalized by initial sample mass. Overall theoretical degree of crystallinity *Xc* was calculated based on the melting enthalpy ($\Delta H_m$) according to the following equation: $Xc = \Delta H_m / \Delta H^0_{PHB}$, where $\Delta H^0_{PHB}$ is the melting enthalpy of pure PHB crystals, i.e. 146 J g$^{-1}$ [10]. In the case of double melting peaks, partial crystallinities $Xc_1$ and $Xc_2$ were calculated for both the first and the second melting enthalpies corresponding to $Tm_1$ and $Tm_2$ ($\Delta H_{m1}$ *and* $\Delta H_{m2}$) as follows: $Xc_x = \Delta H_{mx} / \Delta H^0_{PHB}$. In general case, double peaks were sufficiently separated to calculate respective enthalpies (except for PHBV18% after melting at *Tph* = 160 °C, where only $\Delta H_m$ has been reported).
In parallel, step scan DSC (SDSC) was also used in addition to DSC to separate exothermic phenomena (including crystallization and recrystallization) from glass transition, reversing melting or other heat capacity related events. SDSC analysis was first carried out following the same conditions as DSC. About 10 mg of sample were first heating at *Tph* at 10 °C.min$^{-1}$ (*Tph* = 150 °C and 190 °C for PHBV18%; 180 °C and 220 °C for PHBV3%), then stabilized for 3 min and finally cooled down to -30 °C at 10 °C.min$^{-1}$. SDSC heating scans were also performed from -30 to 190 °C using an average heating rate of 2 °C.min$^{-1}$ and a stabilization step duration of 60 s, i.e. a temperature increment of 1 °C after each stabilization step. The data were normalized by the baseline obtained from an experiment achieved with empty pans following the same thermal cycle. The heat flow data derived from the iso-scan SDSC heating program were used to obtain two curves, i.e. the apparent thermodynamic heat capacity (Cp, ATD) signal (reversible) and the IsoK baseline heat capacity (Cp, IsoK) signal (related to kinetic and non-reversible events). Analyses were done in duplicate.

**Wide and Small Angle X-ray Diffraction (WAXS and SAXS)**

To analyze the evolution of sample crystallinity with thermal treatment, thermo-regulated WAXS (wide angle X-ray scattering) experiments were performed with an in-house setup of the Laboratoire Charles Coulomb, (Université Montpellier, France). A high brightness low power X-ray tube, coupled with aspheric multilayer optic (GeniX$^{3D}$ from Xenocs) was employed. It delivers an ultralow divergent beam (0.5 mrad, λ = 0.15418 nm). Scatterless slits were used to give a clean 0.6 mm beam diameter with a flux of 35 Mphotons/s at the sample. We worked in a transmission configuration and scattered intensity was measured by a 2D "Pilatus" 300K pixel detector by Dectris (490*600 pixels) with pixel size of 172×172 µm$^2$, at a distance of 0.2 m from the sample. Glass capillaries sample holders were used and inserted in an adapted Linkam stage for temperature control. A first scanning routine was set to reproduce a complete DSC scanning thermal cycle (21 °C $T_{m1}$ 21 °C at 10 °C.min$^{-1}$) from which the signal was acquired every 10 °C step.

The crystalline lattice parameters (b, a and c) of the orthorhombic cell [11] were obtained from the position of (0 2 0), (1 1 0) and (1 2 1) reflexions at 13.4°; 16.9° and 25.5° (2θ) respectively, using the following relation (*relation 1*) suitable for an orthorhombic unit cell:

$$d_{hkl} = \frac{1}{\sqrt{\frac{h^2}{a^2}+\frac{k^2}{b^2}+\frac{l^2}{c^2}}} \qquad \text{equation } 1$$

The interplanar distance $d_{hkl}$ was determined using the Bragg law (*relation 2*) which is a function of the X Ray wavelength λ, the values of the Miller indexes (*h k l*), the position (°) and order *n* of the (*nh nk nl*) reflexion:

$$n\lambda = 2d_{hkl}\, sin\, sin\, \theta_{nh\, nk\, nl} \qquad \text{equation } 2$$

The results from our previous work on isothermal behaviour of PHBV3% and PHBV18% raw powders [7] showed that the two products displayed very similar diffractograms, and hence crystalline structures (Figure 1). The crystalline lattice parameters (Table 1) are in good agreement with the results previously reported for PHBV12% [14,15]. ~~The significant increase of a and b, but also of c (chain direction) with increasing HV content indicates that the 3HV unit co-crystallizes into the P(3HB) crystalline lattice, thus expanding and losing the lattice [16].~~ The evolution of the b parameter (around 0.05%) can be attributed to the shift of the plane (020). For a and c paramters, the change between PHBV3% and PHBV18% are not significant, being significantly below the margin of error related to the measurement (0.005 nm). No additional diffraction peak could be observed with increasing HV content, indicating that the HV units did not induce PHBV polymorphs with crystallization according to new crystalline planes. Indeed, the very similar macromolecular structures of PHB and PHV homopolymers is known to result in PHBV exhibiting isodimorphism [13].

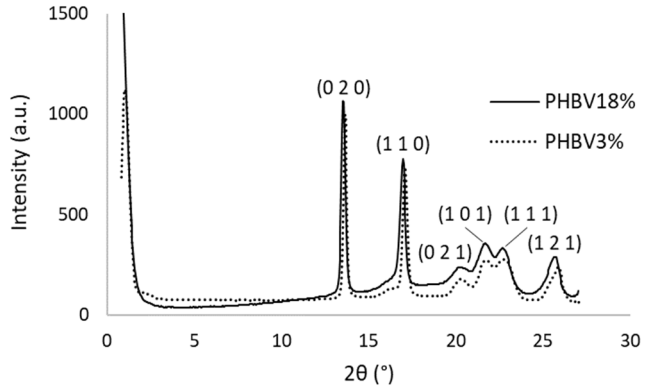


**Figure 1.** (half page) WAXS diffractograms of PHBV3% and PHBV18%. Raw data available at https://doi.org/10.15454/MNEKPC.

In this work, a second analysis was performed to check the evolution of the morphology of final crystals after a preheating at different *Tph*. A unique signal was here acquired after melting at *Tph* and recrystallization to reproduce POM analysis (21 °C ▫ *Tph* ▫ 21 °C at 25 °C.min$^{-1}$), from which signal was acquired at *Tph* and at the end of the cooling step. A new sample was used for each measurement.

**Nuclear Magnetic Resonance (NMR) spectroscopy**

PHBV films (see preparation of the films) were dissolved in deuterated chloroform (CDCl3) to a concentration of 10 mg.mL$^{-1}$ at 60 °C for 12 h, and filtrated with 20 µm PTFE syringes. $^{1}$H and $^{13}$C NMR spectra of the films were carried out on a Bruker spectrometer Ascend III HD operating at 400 MHz for protons and 100 MHz for carbons. The $^{1}$H NMR spectra were recorded at 25 °C, 3 kHz for spectral width, 1600 Hz for transmitter frequency offset, 3 s for acquisition time and 4 scans. Quantitative conditions were obtained with a 30° pulse (3 µs) and a relaxation delay at 1 s (D1). The $^{13}$C NMR

spectra were recorded at 25 °C, 29 kHz for spectral width, 1kHz for transmitter frequency offset, 0.8 s for acquisition time, 4096 scans (NS) with a 30° pulse (3.3 µs) and a relaxation delay at 5 s (D1). $^{1}$H decoupling was applied during acquisition (waltz16 with a pulse of 90 µs). The solvent resonance peak was used as a chemical shift reference at 7.26 ppm for $^{1}$H and 77.0 ppm for $^{13}$C NMR.
The typical peaks of each group according to their chemical displacement are summarized in Table 2 according to our previous work [7], and match with the results found in the literature [13,35,36].

**Table 2.** Position of the $^{13}$C NMR detected peaks and the corresponding copolymer chemical groups.

| | Chemical Group or Specific Peak | Position (+/-0,1ppm) |
|---|---|---|
| CH2 | HB2 | 40.79 |
| | HV2 | 38.81 |
| CH3 | HV4 | 26.86 |
| | HB4 | 19.75 |
| | HV5 | 9.35 |
| Intermediate peaks | Peak X | 31.6 |
| | Peak Y | 22.66 |
| | Peak Z | 14.13 |

**Polarized Optical Microscopy (POM)**
POM observations were performed on a Laborlux 11 POL S (Leitz, Germany) microscope in the transmission mode, equipped with a mono-CCD Leica DFC420 camera (resolution 1728 × 1296 pixels) and piloted by the Archimede® software (Microvision Instruments, France). Each sample was placed between two glass slides, then heated onto a LTS420 hot stage (Linkam, UK) up to *Tph* at 10 °C.min$^{-1}$ and annealed for 3 min before being cooled at 80 °C (at 25 °C.min$^{-1}$) and stabilized 60 min before observation. The crystallization temperature was set to 80 °C since it has been reported that for both PHB and PHBV, it enabled to reach the highest spherulites radial growth [12]. In the case of cold-crystallization, a second step of re-heating was performed up to 150 °C at 10 °C.min$^{-1}$.

**Preparation of PHBV films for mechanical testing**
PHBV films were prepared to further characterize the impact of the macromolecular and crystalline structures on the mechanical performance of the materials. Films with an average thickness of 300 µm were produced from the raw powders by thermocompression using a heated hydraulic press (20T, Pinette Emidecau Industries, Chalon-sur-Saône, France). For each film, the heating plates of the press were first stabilized to a specific processing temperature (from 160 to 220 °C for PHBV3% and from 125 to 160 °C for PHBV18%; with steps of 5 °C) and about 5 g of raw powder was deposited on the plates in a mold, between two Teflon sheets. The pressure was first set to 5 bars for 1 min to melt the powder, then progressively raised from 5 to 150 bars in 30 s before stabilization at 150 bars during 30 s. Films were finally air cooled to room temperature after processing.

**Tensile properties**
ISO½ samples were cut from the films obtained by thermocompression and stabilized during 5 days at 25 °C and 50 %RH prior to testing. Tensile properties were measured on stabilized samples using a tensile tester (Zwick BZ2.5/TN1S, Metz, France) with a cross-head speed of 1 mm.min$^{-1}$. Young's modulus, strain and stress at break as well as energy at break were calculated from strain-stress curves with the Matlab program. Ten replicates were characterized for each formulation.

## RESULTS AND DISCUSSION

### 1. Studying the processing window of PHBV by DSC and thermo-regulated WAXS

A thermo-regulated WAXS analysis was carried out to reproduce the melting DSC cycle (heating at 10 °C.min$^{-1}$ until 180 °C, 3 min of stabilization and cooling at 10 °C.min$^{-1}$) with successive acquisitions recorded every 5 °C. Only the relevant thermograms corresponding to temperatures where changes could be observed are illustrated in Figure 2 for both PHBVs. For PHBV18%, it could be observed that the intensity of all peaks gradually decreased during heating. Also, the low intensity and bell-shaped peaks associated to planes (0 2 1) to (1 2 1) completely disappeared above 150°C, while the two sharp peaks associated to planes (0 2 0) and (1 1 0) disappeared at higher temperatures around 160°C. In contrast, for PHBV3% all peaks disappeared around 185°C, which is in agreement with the sharp crystallization peak observed in DSC.

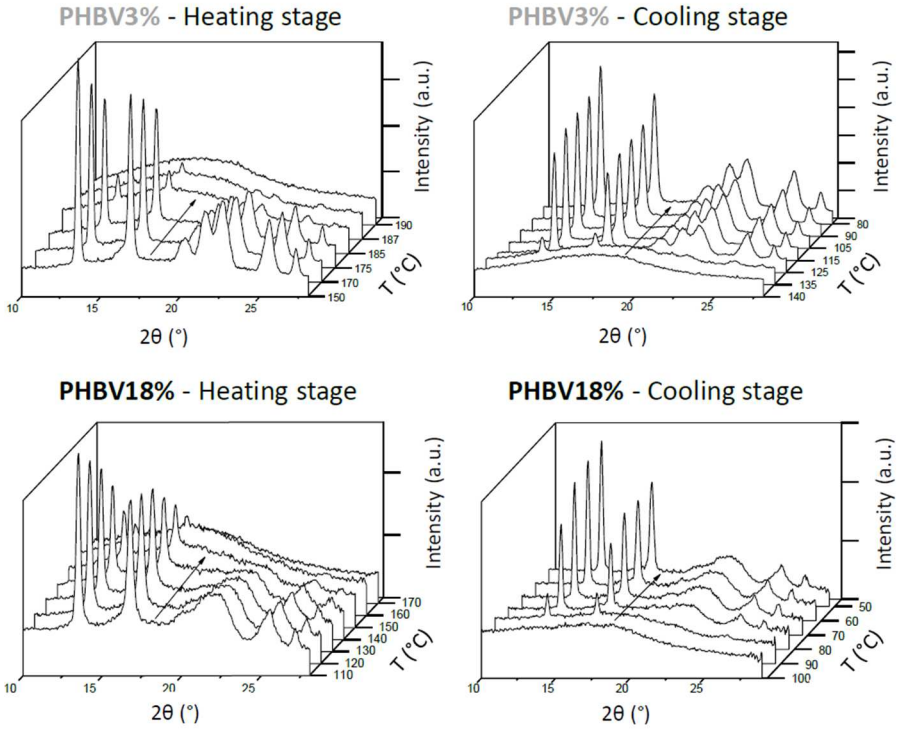


**Figure 2.** (full page) Thermo-regulated WAXS experiments. Evolution diffractograms of PHBV18% (on the bottom) and PHB3% (on the top) with temperature during first heating phase (on the left) and subsequent cooling phase (on the right), reproducing a classic DSC cycle. Raw data available at https://doi.org/10.15454/MNEKPC.

It is worth noting that a shift between melting temperatures deduced from WAXS results (*Tmelt_onset* and *Tmelt_offset* in Table 3) and the ones assessed by DSC could be observed, with melting beginning at higher temperatures in the case of DSC analysis (+11°C in average between $Tm_0$ and *Tmelt_onset*). Such difference was most likely related to the fact that DSC analyses were conducted under an inert atmosphere, whereas WAXS experiments were conducted under oxidative conditions, which are supposed to fasten the reaction.

**Table 3.** Comparison between DSC results from our previous work [7] and values from thermo-regulated WAXS experiments of PHBV3% and PHBV18% obtained in this work: temperatures corresponding to the beginning (Tmelt_onset) and end (Tmelt_offset) of the melting process, according to the disappearance of diffraction peaks on Figure 2).

| | DSC results [7] | Thermo-regulated WAXS results | |
|---|---|---|---|
| | Tm0 (°C) | Tmelt_onset (°C) | Tmelt_offset (°C) |
| PHBV 3% | 174.3 | 185 | 187 |
| PHBV 18% | 138.5 | 150 | 160 |

These results also highlighted the strong interest of thermo-regulated WAXS experiments in the study of polymers melting, since the temperatures at which each specific crystalline form melts can

be analyzed with this method. Finally, it allows concluding that coherent minimal temperatures to be defined as the starting point of the tested thermal treatments should be 150 °C for PHBV18% and 180 °C for PHBV3%.

In order to avoid irreversible thermal degradation during material processing, the choice of the maximal preheating temperatures was defined according to the degradation temperatures of the PHBV grades obtained by thermogravimetric analysis (TGA) under nitrogen [7]. A one-step thermal degradation was observed for both PHBV grades, confirming pure organic compounds. PHBV18% was much less thermally stable than PHBV3%, with weight loss beginning at temperatures approximately 50°C lower than PHBV3% (intersection point of the extrapolated baseline and the inflectional tangent at the beginning of the mass loss, *Tonset* = 219.7 °C and 264.7 °C for PHBV18% and PHBV3%, respectively).

In conclusion, the maximal preheating temperature that could be applied was set to $Tph = Tm_0 + 50$ °C, avoiding thermal degradation in this way. *Tph* was therefore defined to cover the interval [$Tm_0 + 10$ °C, $Tm_0 + 50$ °C] (rounded to the nearest 10 °C), i.e. from 180 to 220 °C for PHBV3% (with steps of 20 °C) and from 150 to 190 °C for PHBV18% (with steps of 10 °C, due to lower thermal stability).

**2. Effect of hydroxyvalerate content on the non-isothermal crystallization and melting behaviors**

Figure 3 and Figure 4 present the DSC thermograms obtained for PHBV3% and PHBV18% after preheating at the different *Tph* as defined in the previous section. The thermograms recorded for the cooling phase from *Tph* to -30 °C (A) and the second heating phase from -30 °C to 190 °C (B) are displayed. The measured crystallization and melting temperatures, and calculated enthalpies and crystallinity degrees are given in Table 4.

*a. Effect of the preheating temperature on the crystallization behavior*

For both PHBVs, increasing *Tph* resulted in a pronounced decrease of the melt crystallization temperature (*Tc*). In the case of PHBV3%, *Tc* shifted from 121 °C to 80.5 °C and 76.5 °C after preheating at 180 °C, 200 °C and 220 °C, respectively. In the case of PHBV18%, *Tc* also gradually decreased from 106.4 °C to 73.4 °C, for preheating increasing from 150 °C to 180 °C. Such a shift of *Tc* with increasing *Tph* was previously observed for PHB [8,23]. Increasing *Tph* allowed eliminating all residual nuclei in the melt, with no preferential nucleation sites, making it more difficult to reach a new ordered system. As a result, the formation of nuclei and the crystallization process starts at lower temperatures.

It is also interesting to discuss the shape of the melt crystallization peak. For PHBV3%, for *Tph* = 180 °C, a sharp crystallization peak was observed at 121 °C, indicating that a unique family of crystal planes formed from the melt due to self-nucleation. Melting conditions were thus adequate. After a preheating at *Tph* = 200 °C, the crystallization peak was less sharp and double-humped shaped, which suggested the coexistence of different crystal types. For PHBV18%, *for Tph* = 150 °C, the melt crystallization peak was bell-shaped and of small intensity. Previous WAXS experiments indicated that a preheating at 150 °C was not sufficient to erase the thermal history of the sample. Such a bell-shape crystallization peak might result from the superposition of new created crystals and crystals formed from the remaining unmelted crystals. While *Tph* increased up to 170 °C, the melt crystallization peak intensity increased and got sharper. WAXS experiments showed that above *Tph* = 160 °C, a complete melting of the polymer with no residual nuclei is achieved. The intensification of the crystallization peak from *Tph* = 150 to 170 °C could thus be explained by the fact that a more homogeneous crystal phase was produced from the melt in that case. Above *Tph* = 180 °C, the melt crystallization enthalpy decreased again, and for *Tph* = 190 °C no melt crystallization peak at all could be observed.

**Table 4.** Crystallization and melting parameters obtained from non-isothermal crystallization DSC curves for PHBV3% and PHBV18% after a first preheating at different temperatures *Tph*. *Tc*: temperature of melt crystallization; *Tcc*: temperature of cold-crystallization; *ΔHc*: crystallization enthalpy; *ΔHcc*: cold crystallization enthalpy; *Tg*: glass transition temperature; $Tm_1$: unique or first melting temperature peak; $Tm_2$: second melting temperature peak; $\Delta Hm_i$ and $Xc_i$: melting enthalpy and crystallinity based on $Tm_i$; *Total_ΔHm* and *Total_Xc*: overall enthalpy and overall crystallinity based on the integration of all melting peaks together.

| | ***Tph*** | *Tc* | *Tcc* | *ΔHc* | *ΔHcc* | *Tg* | *Tm1* | *ΔHm1* | *Xc1* | *Tm2* | *ΔHm2* | *Xc2* | *ΔHm* | *Xc* |
|---|---|---|---|---|---|---|---|---|---|---|---|---|---|---|
| | °C | °C | °C | J/g | J/g | °C | °C | J/g | % | °C | J/g | % | *J/g* | *%* |
| **PHBV3%** | **180** | 121.02 | - | 81.35 | | 1.23 | 175.64 | *84.37* | *58* | - | - | - | *84.37* | *58* |
| | **200** | 80.57 | - | 63.76 | | 0.82 | 169.86 | *84.82* | *58* | - | - | - | *84.82* | *58* |
| | **220** | 76.49 | - | 64.78 | | 0.62 | 158.49 | *15.11* | *10* | 169.87 | *60.98* | *42* | *76.09* | *52* |
| **PHBV18%** | **150** | 106.35 | - | 29.24 | | -6.58 | 142.9 | *43.72* | *30* | 161.3 | *3.5* | *2* | *51.12* | *35* |
| | **160** | 101.64 | - | 41.21 | | -6.44 | 142.67 | - | - | 151.93 | - | - | *50.38* | *35* |
| | **170** | 97.45 | - | 47.3 | | -6.74 | 139.37 | *46.09* | *32* | 149.66 | *7.28* | *5* | *54.08* | *37* |
| | **180** | 73.42 | - | 46.32 | | -6.85 | 126.46 | *17.25* | *12* | 142.1 | *37.47* | *26* | *54.72* | *37* |
| | **190** | - | 50.01 | - | 40.1 | -7.03 | 113.25 | *8.44* | *6* | 135.02 | *45.65* | *31* | *54.09* | *37* |

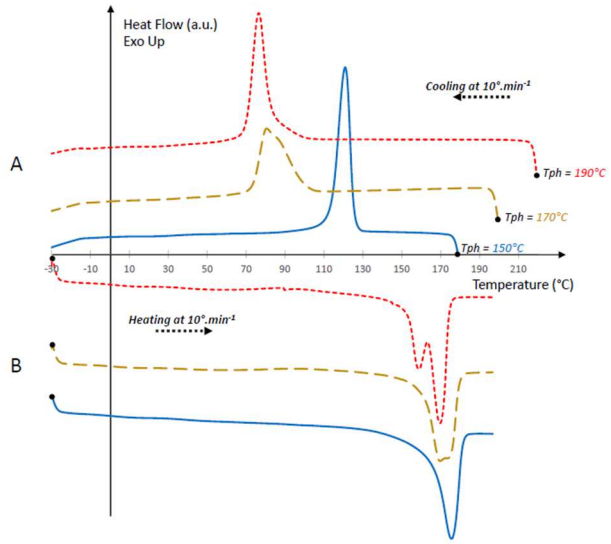


**Figure 3.** (half page) DSC thermograms obtained for PHBV3% after a preheating step during 3 min at various temperatures from *Tph* = 180 to 220 °C. A: identification of crystallization peaks during the cooling scan from *Tph* to -30 °C; B: identification of melting peaks during the second heating scan from -30 °C to 190 °C. Raw data available at https://doi.org/10.15454/MNEKPC.

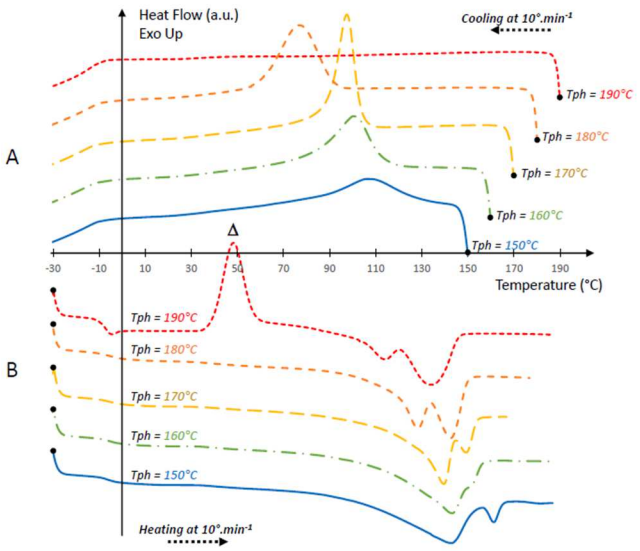


**Figure 4.** (half page) DSC thermograms obtained for PHBV18% after a preheating step during 3 min at various temperatures from *Tph* = 150 to 190 °C. A: identification of crystallization peaks during the cooling scan from *Tph* to -30 °C; B: identification of melting peaks during the second heating scan from -30 °C to 190 °C; Δ symbol indicates cold crystallization peak. Raw data available at https://doi.org/10.15454/MNEKPC.

*b. Effect of the preheating temperature on the re-melting behavior*

Increasing the preheating temperature induced the apparition of a double melting peak in PHBV3% above *Tph* = 200 °C. For PHBV18%, double melting peaks were observed in all cases. Another important feature observable for PHBV18% for *Tph* = 190 °C is the apparition of a cold crystallization peak during the second heating step (at *Tcc* = 50 °C, Figure 4B). Cold crystallization events have already been observed for PHBV with HV content superior to 10 % [15,18]. This supported the hypothesis of the coexistence of different crystals forms with varying thermal stability and hence various melting temperatures.

Based on all these observations, the double melting peaks observed on the second heating scans for PHBV3% and PHBV18% could be the manifestation of segregation (separation between different crystal forms) and/or melting-recrystallization processes. To better depict the origins of double melting peaks, step-scan DSC (SDSC) analysis has been performed to enable the separation of exotherms of crystallization events that can be hidden by glass transition, melting or other heat capacity related events (see Supplementary Material). After conditioning at the lowest *Tph*, for both PHBV3% (i.e. *Tph* = 180 °C) and PHBV18% (i.e. *Tph* = 150 °C), no melting/recrystallization event was observed. The double melting peak always observed on thermograms of PHBV18% should thus be related to the existence of two different crystal populations having different melting temperature. After conditioning at higher preheating temperature, melting-recrystallization was only observed for PHBV3% (at 163 °C). For PHBV3%, the preheating at *Tph* = 220 °C thus induced the formation of crystals of varying stability: the first and second melting peaks can reasonably be attributed to the melting of the most stable crystals and the melting of crystals formed through the melting-recrystallization process, respectively. For PHBV18%, no melting-recrystallization was observed for *Tph* = 190 °C, but a small exothermic peak was observed at low temperature (24 °C), confirming the existence of a cold crystallization event.

*c. Relationships between macromolecular structures and the effect of preheating temperature on thermal behavior of PHBV*

As mentioned in the introduction, it was proposed in the literature that HB-rich domains, having higher melting temperature, could be more or less miscible with HV-rich domains, having lower melting temperature [30]. Thus, the existence of double melting peaks observed on thermograms

(Figure 3B and 4B) could be reasonably attributed to the melting of PHB-rich and PHV-rich crystal populations. Also, since PHV crystallizes at lower temperature compared to PHB [31], melting peaks occurring at the lowest and highest temperatures can be attributed to PHV-rich and PHB-rich domains, respectively. On this basis, DSC results can thus be analyzed in relation with macromolecular structures to discuss the effect of preheating on the composition of the obtained crystals.

For PHBV3%, when melting is performed at low temperature (*Tph* = 180 °C), co-crystallization of PHV-rich and PHB-rich domains is properly achieved. Then, at a certain critical temperature (*Tph* = 200 °C), a segregation of PHV-rich and PHB-rich domains occurs but co-crystallization can still occur; finally, above this critical temperature (*Tph* = 220 °C), PHB-rich and PHV-rich crystal populations could be not miscible anymore, leading to the apparition of a clear double melting peak (the lowest melting peak being attributed to less stable crystals which recrystallize during re-heating, as identified in SDSC - see Supplementary Material). For PHBV18%, previous results showed that melting peaks are observed for all preheating conditions and not related to melting-recrystallization phenomenon. PHBV18% is a block-copolymer with macromolecular chains consisting in a succession of PHB and PHV blocks characterized by different crystallization behaviors [7]. During crystallization process, the evolution of the microstructure in block copolymer systems has been proved to be the result of two competing phenomena: (i) segregation of dissimilar blocks due to their inherent incompatibility and (ii) segregation being limited spatially by the connectivity of the blocks imposed by the architecture of the macromolecules and the molecular mobility. Phase segregation competes with co-crystallization giving rise to the formation of phase structures that vary with the miscibility of the component copolymers [32]. This specific structure explains the aspect of the melting curves observed, the lowest and highest temperature peaks possibly being attributed to the chains having a larger number of HV blocks or HB blocks, respectively. For PHBV18%, the increase of *Tph* up to 180 °C resulted in gradual increase of melting temperatures and separation between Tm1 and Tm2. This could correspond to the progressive segregation of HV- and HB-rich chains, leading to a higher polycrystallinity (confirmed by the bell shape aspect of the crystallization peak in Figure 4A). Indeed, the intensity of the melting peak occurring at the highest temperature (HB-rich domains) increased with *Tph* (*ΔHm2* increased from 3.5 to 45.6 $J.g^{-1}$, when *Tph* increased from 150 to 190 °C) at the expense of the one occurring at lower temperature (HV-rich domains) (*ΔHm1* decreased from 43.72 to 8.44 $J.g^{-1}$, when *Tph* increased from 150 to 190 °C). It is thus likely that a higher temperature of preheating would favor PHB-rich domain crystallization at the expense of PHV-rich domain.

Finally, at *Tph = 190 °C*, the large amount of separated PHV-rich material in the melt cannot crystallize anymore upon cooling (Figure 4A) and remain amorphous, resulting in the apparition of a cold-crystallization upon the second heating scan (Figure 4B). This hypothesis is supported by the fact that preheating of PHBV18% at *Tph* = 190 °C led to the apparition of (i) a glass transition temperature and (ii) a cold-crystallization peak typical of pure rigid amorphous PHV material, as shown by Wang et al. (2011). As a result, after melting at high *Tph*, the favoring of PHB-rich domains' crystallization and the larger share of rigid amorphous phase due to PHV-rich domains are expected to negatively impact the final mechanical properties. Cheng et al. (2009) studied PHBV with a valerate content of 5 mol% by DSC coupled to positron annihilation lifetime spectroscopy. The authors showed that, for the same overall crystallinity, cold-crystallized crystals of PHBV contained a larger amount of interlamellar rigid amorphous fraction and smaller domain size of the inter-stack mobile amorphous phase than melt-crystallized crystals, resulting in more rigid materials [33]. The temperature processing window for PHBV18% is therefore very limited, i.e. (i) too low preheating temperatures resulted in uncompleted melting where remaining unmelted structures lead to the formation of inhomogeneous crystals, and (ii) too high preheating temperatures resulted in a cold-crystallization phenomenon and less flexible materials.

These results highlight that processing temperatures should be carefully adapted to each type of PHBV copolymer. The crystallization behavior of PHBV and their final microstructure can be tuned by controlling the thermal cycle of preheating and cooling during processing. Here, a more detailed

study of the morphology of the different studied crystals is needed to verify if segregation actually occur depending of melting conditions, as deduced from DSC analysis.

### 3. Impact of the preheating temperature on the crystalline and molecular structure of PHBV

Polarized Optical Microscopy (POM) analysis has been conducted to observe the final crystalline structure of PHBV obtained from the melt after a preheating at different temperatures, using same conditions as for non-isothermal DSC experiments, i.e. samples were first heated up to *Tph* at 10 °C.min$^{-1}$ and annealed for 3 min, before being cooled down to the isothermal crystallization temperature fixed at 80 °C (25 °C.min$^{-1}$) and stabilized 60 min before observations. This analysis revealed that, for both copolymers, different crystalline structures were formed from the melt depending on *Tph*.

For PHBV3% melted at low temperature (*Tph* < 190 °C), and homogeneous crystalline structure with small spherulites of about 5 µm was obtained (Figure 5A and 5B). In these conditions, complete melting and co-crystallization was achieved, in agreement with the single melting peak previously observed in DSC thermograms. At *Tph* = 200 °C, the crystalline structure was completely different, i.e. characterized by large spherulites of about 430 µm (Figure 5C) having a morphology close to the one obtained for pure PHB when observed in similar isothermal crystallization conditions [34]. For *Tph* > 200 °C, different morphologies with some extremely large PHB-like crystals (of about 620 µm) and smaller ones (of about 190 to 330 µm) were observed (Figure 5D and 5E), supporting the hypothesis of HB-rich and HV-rich units' segregation. This is also consistent with the apparition of a double melting peak in DSC thermograms. For PHBV18%, at *Tph* = 150 °C, POM images showed a heterogeneous crystalline structure (Figure 5F), confirming that melting was incomplete in these conditions, as also inferred from the bell aspect of the melting peak observed in DSC (Figure 4B) and the remaining crystalline structures observed on the thermo-regulated WAXS experiments (Figure 2). Here, part of the crystals might have been formed from the partially ordered crystalline phases remaining in the sample because thermal history of the sample was not completely erased. For *Tph* ranging from 160 to 170 °C, homogeneous crystalline structures are observed (crystals diameter being around 5 µm at *Tph* = 170 °C), indicating suitable melting conditions. This observation is consistent with the conclusions taken from the DSC results, where the best melting conditions were identified for *Tph* = 170 °C. For *Tph* = 180 °C, an increase of crystals size is observed (Figure 5I) (crystals diameter being around 40 µm), which is most likely related to the progressive segregation of PHB-rich domains, forming bigger crystals. Finally, for *Tph* = 190 °C, crystallization is uncompleted and a large region of the melt remains amorphous, even after 60 min at 80 °C (Figure 5J). This explained the absence of crystallization peak observed during cooling in DSC (Figure 4A). It is only during reheating that the amorphous zone partially recrystallizes through a cold-crystallization process as measured on DSC thermograms (Figure 4B) and observed by POM (Figure 5Jbis).

These observations prove that the cold-crystallization phenomenon observed for highly pre-heated samples originates from the recrystallization of rigid amorphous PHV-rich domains during re-heating.

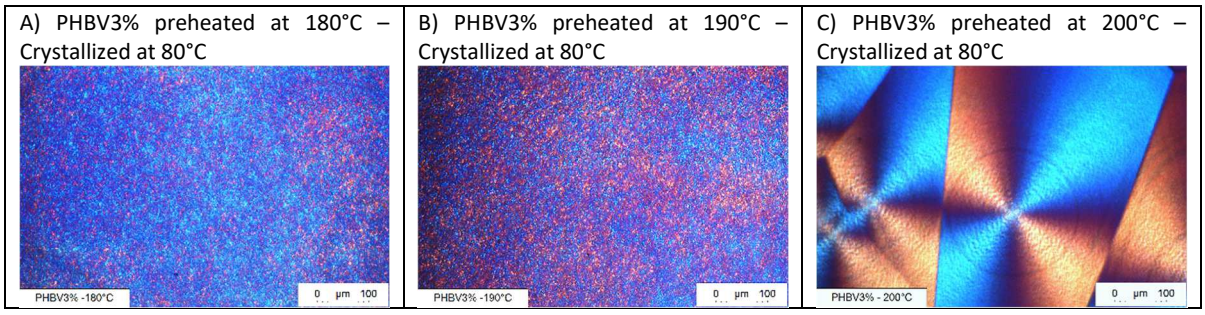

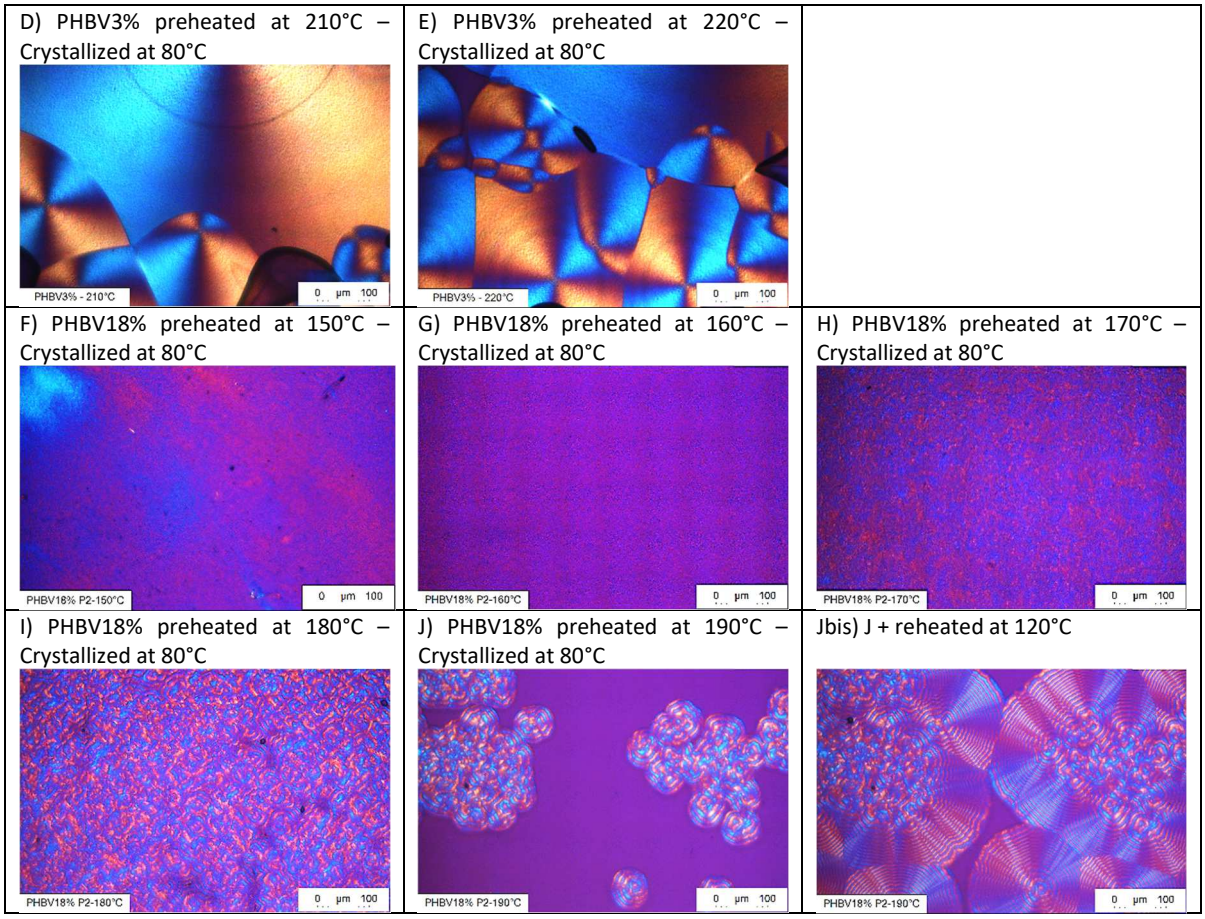


**Figure 5.** (full page) POM images of PHBV3% (A to E) and PHBV18% (F to J) after heating to varying *Tph* (at 10 °C.min$^{-1}$), quick cooling at 80 °C (at 25 °C.min$^{-1}$) and 60 min of stabilization. For PHBV18% melted at *Tph* = 190 °C, the sample was subsequently reheated at 120 °C to observe the cold crystallization (J).

Then, in order to track the influence of the preheating temperature on the crystalline structure, thermo-regulated WAXS experiments have been performed. Measurements were conducted on samples after heating up to *Tph* and crystallization at 20 °C. *Tph*-dependent diffractograms are shown in Figure 6. For PHBV18%, it can clearly be seen that there exists a critical *Tph* at which the copolymer is not able to recover its original crystalline structure after cooling. Indeed, when preheating PHBV18% samples at 180 °C and 190 °C, the baseline of the WAXS diffractogram is displaced to higher intensity and the low-crystalline structures, corresponding to planes (0 2 0) and (1 1 0) and attributed to PHV-rich domains, are not visible anymore. Above 180 °C, a part of the copolymer remains amorphous even after cooling to room temperature. These results confirmed that PHV-rich regions cannot crystallize anymore after high preheating treatments, as previously inferred from DSC and POM analysis. This also better specifies the critical temperature at which the phenomenon starts to occur, i.e. *Tph* = 180 °C. For PHBV3%, only little differences can be observed compared to the unmelt powder, independently of *Tph*. Here, even if the thermal treatment is likely to result in the segregation of different crystals forms, the crystallization is totally completed (with similar diffractograms) whatever the *Tph*. Despite having similar crystalline patterns, it is important to point out that the size of spherulites is strongly affected by *Tph*, which should have an effect on the final mechanical properties of the copolymer.

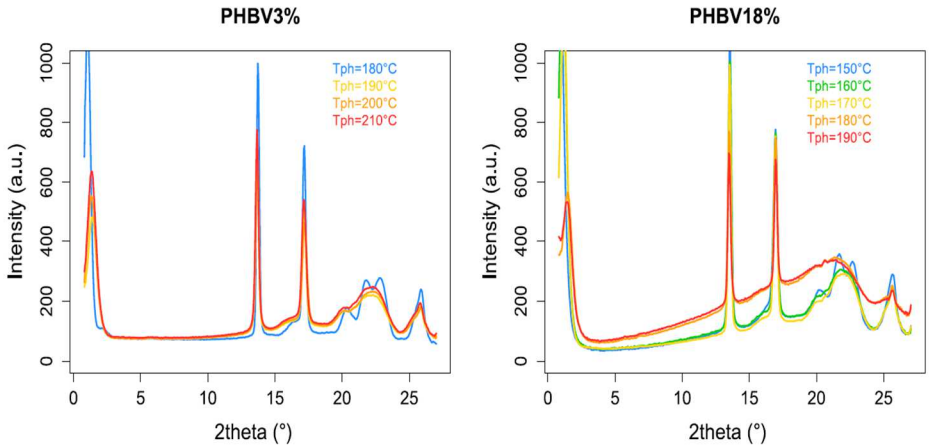


**Figure 6.** (0.75page) WAXS diffractograms obtained after melting at various *Tph* and crystallization at 21°C during 60 min. PHBV18% (A) and PHBV3% (B). Raw data available at https://doi.org/10.15454/MNEKPC.

NMR characterization has been carried out on PHBV18% films processed near the minimal and maximal temperatures enabling films to be properly produced, i.e. at 135 °C and 150 °C. The obtained $^{13}C$ spectra have been compared to the one of PHBV18% raw powder (Figure 7). Each peak observed was assigned to a specific monomer unit of the copolymer structure (*HBi* or *HVi*, *i* being the carbon number, are the different monomer units present in the copolymer structure, as illustrated in the top right corner of Figure 7).

For the PHBV18% raw powder sample, intermediate peaks were observed (*X*, *Y* and *Z* peaks in Figure 7) between the specific peaks attributed to HB and HV units. Indeed, if no thermal degradation has occurred, PHB-rich and PHV-rich domains are formed with no macrophase separation and their dimensions is related to the length of the different units. In that case, these specific signals are observed and constitute markers of the interactions between PHB and PHV units [7]. The X, Y and Z peaks were observable for films processed until 135 °C, but disappeared for films processed at 150 °C. This information confirmed that at a certain critical temperature, thermal degradation occurred and induced a loose of interaction between PHB-rich and PHV-rich domains in the copolymer. It explained the origin of the gradual crystals segregation observed previously in DSC and POM analyses. We can assume that an increase in preheating temperature is unfavorable to co-crystallization. These findings suggested that high temperatures modify intermolecular interactions between the copolymer's chains.

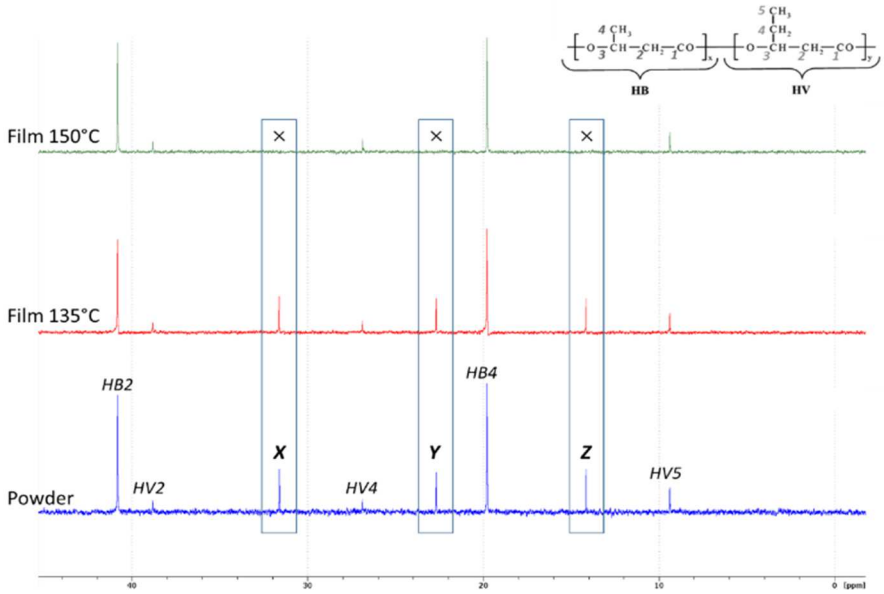

**Figure 7.** (half page) $^{13}C$ NMR spectra of PHBV18% raw powder and thin films realized at 135 °C and 150 °C.

## 4. Impact of the preheating temperature on processability and mechanical properties of PHBV-based films

In order to analyse the effect of the structural changes and thermally-induced degradation previously reported on processability and mechanical properties of PHBV, thin films with an average thickness of 300 µm were formed from the raw PHBV powders using a heating hydraulic press. From a technical point of view, these results also aim at defining the practical processing window of the studied copolymers for their implementation in packaging applications.

### *a. Processability of PHBV-based films*

Because films were formed under high pressure conditions (150 bars), it was likely that their thermal sensitivity could differ from the one reported in DSC and POM analyses. Therefore, a broader variability of processing temperatures with smaller temperature steps (every 5°C) has been used for the production of films compared to previous analyses. Based on visual assessment, the processability of the films depending on melting conditions is illustrated in Figure 8. Three cases were defined: unmelt, when agglomerates of unmelt powder were still visible; processable, when powder was correctly melted and films showed no cracks; unprocessable when films did not crystallize, or crystallize but showed cracks. The results revealed a processing window ranging from 175 °C to 210 °C for PHBV3%, which appeared to be similar to the one inferred from DSC. For PHBV18%, surprisingly, the obtained processing window ranged from 130 °C to 150 °C, which was below expectations. Indeed, previous results indicated that proper melting conditions were reached above 150 °C. Here, films could only be properly processed at lower operating temperatures, from 130 °C to 150 °C maximum. In addition, degradations occurred at 160 °C while DSC results suggested a critical temperature of 180 °C. This shift to lower processing temperatures compared to DSC (performed under inert atmosphere) could originate from the oxidative atmosphere. The combined effect of temperature and pressure may also have a marked effect on melting behaviour of PHBV18%.

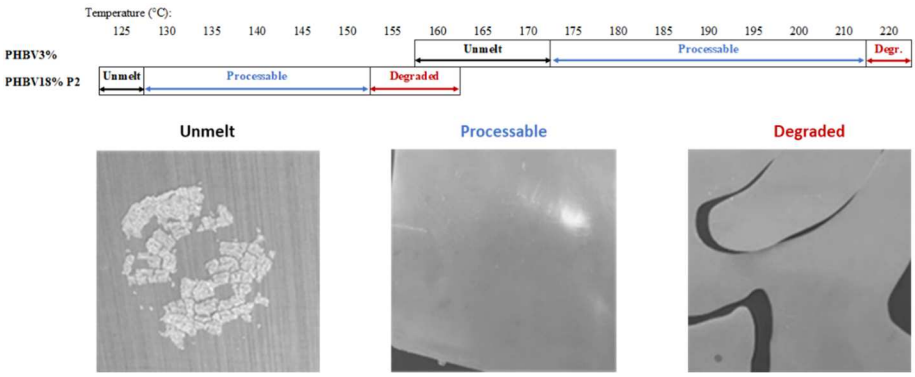


**Figure 8.** (0.75 page) Processability of films (300 µm) obtained from raw powder of PHBV3% and PHBV18% with a heating hydraulic press as a function of operating temperatures.

### *b. Impact of the processing temperature on the mechanical properties of PHBV-based*

All the films showing no macroscopic defect (i.e. “processable” films as defined in Figure 8; plus, an additional set of samples from the degraded PHBV3% film processed at 220°C that could have been cut in the area between cracks) have been mechanically tested under tensile loading. Variations in Young’s modulus, and stress and strain at break as a function of the processing temperature are illustrated for both PHBV3% and PHBV18% in Figure 9.

First, at the minimal processing temperature (respectively 175 and 130 °C for PHBV3% and PHBV18%), the Young's modulus of PHBV18% was much lower compared to PHBV3% (1.18 and 2.28 GPa for PHBV18% and PHBV3%, respectively). Increasing HV content from 3 % to 18 % is indeed expected to soften the copolymer due to higher steric hindrance of PHV units inducing a decrease of overall crystallinity, and hence lower stiffness. It clearly appeared that increasing processing temperature had a strong impact on all the tensile mechanical properties for both polymers.

For PHBV18%, increasing the processing temperature induced a progressive increase of the Young's modulus. The stiffening of the material could be explained by the formation of PHB-rich big crystals from the melt, while PHV-rich domains were progressively isolated and remained amorphous. Regarding stress and strain at break values, low variations were observed between 130 and 145 °C. Beyond, a pronounced decrease of ultimate properties was observed (the strain at break decreased from 3.23 to 1.68 % while the stress at break decreased from 23.49 to 17.47 MPa between 145 and 150 °C). The critical temperature of 145 °C defined for optimal mechanical performance of PHBV18% is consistent with (i) the previous conclusions from NMR analysis, supporting that interactions between PHB and PHV units disappeared at 150 °C (Figure 7) and (ii) with the maximal temperature of processability established from film forming illustrated in Figure 8. It should be pointed out that other degradation phenomena might be involved when processing high-HV content PHBV. In particular, DSC experiments were conducted under nitrogen atmosphere, which might explain why a shift to lower critical processing temperatures was observed for hot-pressing (conducted under ambient atmosphere with probable oxidative effects) compared to critical temperatures deduced from DSC thermograms.

For PHBV3%, increasing processing temperature also resulted in a progressive but less marked increase of the Young's modulus until 200 °C. From 200 to 220 °C, a marked decrease of the Young's modulus was reported, but it is necessary to remind that the film processed at 220 °C was originally considered as unprocessable due to the presence of cracks (samples have been cut within the zone showing no cracks). Here it is clear that 220 °C induced a strong degradation of the polymer and molar mass could have been largely impacted. The high standard deviation measured for these samples also showed that highly variable results were obtained. Regarding ultimate properties, as observed for PHBV18%, passing a critical temperature (200 °C in the case of PHBV3%), a large decrease of performances was observed (strain at break and stress at break passing respectively from 1.39 to 0.79 % and from 27.88 to 14.36 MPa between 200 and 220 °C). This loss of mechanical performance was even more pronounced than the one observed for PHBV18%. In the case of PHBV3%, the critical temperature inferred from mechanical testing of thin films matched the one reported from DSC and POM analyses. Finally, these last experiments proved the need to extend the characterization of the polymers until real mechanical testing of final formed materials to define a realistic processing window in relation with functional properties of the films. In that case, the processing window could be refined to [175; 200 °C] in the case of PHBV3% and [130; 145 °C] in the case of PHBV18%.

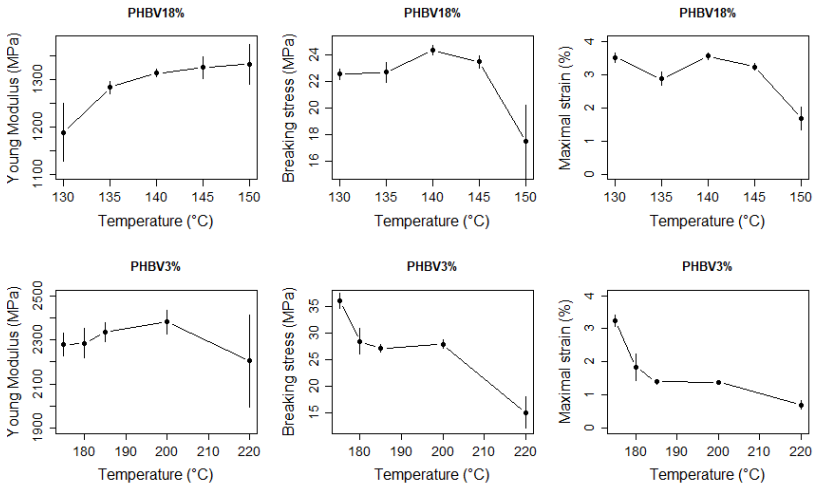


**Figure 9.** (0.75 page) Evolution of the mechanical properties of the thin films realized from PHBV18% (top) and PHBV3% (bottom) raw powders, depending on the processing temperature used in the hydraulic press (150 bars being the maximal pressure applied). Raw data available at https://doi.org/10.15454/MNEKPC.

## CONCLUSIONS

Studying two different grades of PHBV having 3 and 18% of HV units, the purpose of this work was to investigate the influence of the processing temperature on the PHBV macromolecular and crystalline structures, depending on its HV content, and to define a processing window guarantying optimized mechanical properties of PHBV films.

The coupling of differential scanning calorimetry (DSC) and thermogravimetric analysis (TGA) allowed us to define the window of processing temperature to be tested. Then, the thermo-regulated wide angle X-ray (WAXS) analysis appeared to be of great interest to accurately characterize the melting behavior of the studied PHBVs. Our results showed that increasing processing temperature promoted the crystallization of PHB-rich domains and isolation of PHV-rich domains. For PHBV with a HV content of 18 mol%, 180°C was identified as the critical temperature above which PHV-rich domains could not crystallize anymore during cooling and remained amorphous. Finally, mechanical tests performed on films processed through thermal pressing at varying temperatures showed that the thermally-induced changes previously reported led to a marked loss of the material's mechanical performance.

The combination of these experiments enabled to define a realistic processing window, in terms of thermal treatment, for both PHBVs (i.e. [175; 200 °C] in the case of PHBV3% and [130; 145 °C] in the case of PHBV18%). However, the temperatures identified in this work might be overestimated since they do not account for additional self-heating effects resulting from others processing parameters such as pressure for example.

Finally, this work revealed that when increasing the overall HV content of the copolymer, adjusting the processing routine according to these results is critical to match the functional properties targeted for a specific use. It is particularly crucial in the case of such thermally-sensitive biopolymers displaying narrow adequate processing windows, and that care attention should be thus paid by plastics processing industries not to degrade their final performance.

**ACKNOWLEDGMENTS**

This project has received funding from the European Union's Horizon 2020 research and innovation program under grant agreement No 773375.

**REFERENCES**

[1] X. Gao, J.-C. Chen, Q. Wu, G.-Q. Chen, Polyhydroxyalkanoates as a source of chemicals, polymers, and biofuels, Curr. Opin. Biotechnol. 22 (2011) 768–774. https://doi.org/10.1016/J.COPBIO.2011.06.005.

[2] S. Chanprateep, Current trends in biodegradable polyhydroxyalkanoates, J. Biosci. Bioeng. 110 (2010) 621–632. https://doi.org/10.1016/J.JBIOSC.2010.07.014.

[3] C. Pérez-Rivero, G. Hernandez-Raquet, Polyhydroxyalcanoates : une alternative "bio" aux plastiques traditionnels, Université de Toulouse, 2017. https://hal.archives-ouvertes.fr/hal-01669399 (accessed April 11, 2019).

[4] E. Bugnicourt, P. Cinelli, A. Lazzeri, V. Alvarez, Polyhydroxyalkanoate (PHA): Review of synthesis, characteristics, processing and potential applications in packaging, Express Polym. Lett. 8 (2014) 791–808. https://doi.org/10.3144/expresspolymlett.2014.82.

[5] L.S. Serafim, P.C. Lemos, C. Torres, M.A.M. Reis, A.M. Ramos, The influence of process parameters on the characteristics of polyhydroxyalkanoates produced by mixed cultures, Macromol. Biosci. 8 (2008) 355–366. https://doi.org/10.1002/mabi.200700200.

[6] E. Žagar, A. Kržan, G. Adamus, M. Kowalczuk, Sequence distribution in microbial poly(3-hydroxybutyrate-co-3-hydroxyvalerate) co-polyesters determined by NMR and MS, Biomacromolecules. 7 (2006) 2210–2216. https://doi.org/10.1021/bm060201g.

[7] J. Bossu, H. Angellier-Coussy, C. Totee, M. Matos, M. Reis, V. Guillard, Effect of the Molecular Structure of Poly(3-hydroxybutyrate-co-3-hydroxyvalerate) (P(3HB-3HV)) Produced from Mixed Bacterial Cultures on Its Crystallization and Mechanical Properties., Biomacromolecules. (2020). https://doi.org/10.1021/acs.biomac.0c00826.

[8] A. El-Hadi, R. Schnabel, E. Straube, G. Müller, M. Riemschneider, Effect of melt processing on crystallization behavior and rheology of poly(3-hydroxybutyrate) (PHB) and its blends, Macromol. Mater. Eng. 287 (2002) 363–372. https://doi.org/10.1002/1439-2054(20020501)287:5<363::AID-MAME363>3.0.CO;2-D.

[9] R. Renstad, S. Karlsson, A.C. Albertsson, Influence of processing parameters on the molecular weight and mechanical properties of poly(3-hydroxybutyrate-co-3-hydroxyvalerate), Polym. Degrad. Stab. 57 (1997) 331–338. https://doi.org/10.1016/S0141-3910(97)00028-1.

[10] P.J. Barham, A. Keller, E.L. Otun, P.A. Holmes, Crystallization and morphology of a bacterial thermoplastic: poly-3-hydroxybutyrate, J. Mater. Sci. 19 (1984) 2781–2794. https://doi.org/10.1007/BF01026954.

[11] L. Miao, Z. Qiu, W. Yang, T. Ikehara, Fully biodegradable poly(3-hydroxybutyrate-co-hydroxyvalerate)/poly(ethylene succinate) blends: Phase behavior, crystallization and mechanical properties, React. Funct. Polym. 68 (2008) 446–457. https://doi.org/10.1016/j.reactfunctpolym.2007.11.001.

[12] A.J. Owen, J. Heinzel, Ž. Škrbić, V. Divjaković, Crystallization and melting behaviour of PHB and PHB/HV copolymer, Polymer (Guildf). 33 (1992) 1563–1567. https://doi.org/10.1016/0032-3861(92)90139-N.

[13] N. Kamiya, M. Sakurai, Y. Inoue, C. Riichirô, Y. Doi, Studies of Cocrystallization of Poly(3-hydroxybutyrate-co-3-hydroxyvalerate) by Solid-State High-Resolution 13C NMR Spectroscopy and Differential Scanning Calorimetry, Macromolecules. 24 (1991) 2178–2182. https://doi.org/10.1021/ma00009a006.

[14] Y. Hirota, N. Yoshie, N. Ishii, K. Kasuya, Y. Inoue, Correlation between Solid-State Structures and Enzymatic Degradability of Cocrystallized Blends, Macromol. Biosci. 5 (2005) 1094–1100. https://doi.org/10.1002/mabi.200500133.

[15] E. Ten, L. Jiang, M.P. Wolcott, Crystallization kinetics of poly(3-hydroxybutyrate-co-3-hydroxyvalerate)/cellulose nanowhiskers composites, Carbohydr. Polym. 90 (2012) 541–550. https://doi.org/10.1016/J.CARBPOL.2012.05.076.

[16] Y. Wang, S. Yamada, N. Asakawa, T. Yamane, N. Yoshie, Y. Inoue, Comonomer compositional distribution and thermal and morphological characteristics of bacterial poly(3-hydroxybutyrate-co-3-hydroxyvalerate)s with high 3-hydroxyvalerate content, Biomacromolecules. 2 (2001) 1315–1323. https://doi.org/10.1021/bm010128o.

[17] Q.S. Liu, M.F. Zhu, W.H. Wu, Z.Y. Qin, Reducing the formation of six-membered ring ester during thermal degradation of biodegradable PHBV to enhance its thermal stability, Polym. Degrad. Stab. 94 (2009) 18–24. https://doi.org/10.1016/j.polymdegradstab.2008.10.016.

[18] S. Modi, K. Koelling, Y. Vodovotz, Assessing the mechanical, phase inversion, and rheological properties of poly-[(R)-3-hydroxybutyrate-co-(R)-3-hydroxyvalerate] (PHBV) blended with poly-(l-lactic acid) (PLA), Eur. Polym. J. 49 (2013) 3681–3690. https://doi.org/10.1016/J.EURPOLYMJ.2013.07.036.

[19] S.-D. Li, P.H. Yu, M.K. Cheung, Thermogravimetric analysis of poly(3-hydroxybutyrate) and poly(3-hydroxybutyrate-co-3-hydroxyvalerate), J. Appl. Polym. Sci. 80 (2001) 2237–2244. https://doi.org/10.1002/app.1327.

[20] S.-D. Li, J.-D. He, P.H. Yu, M.K. Cheung, Thermal degradation of poly(3-hydroxybutyrate) and poly(3-hydroxybutyrate-co-3-hydroxyvalerate) as studied by TG, TG-FTIR, and Py-GC/MS, J. Appl. Polym. Sci. 89 (2003) 1530–1536. https://doi.org/10.1002/app.12249.

[21] K.J. Kim, Y. Doi, H. Abe, Effects of residual metal compounds and chain-end structure on thermal degradation of poly(3-hydroxybutyric acid), Polym. Degrad. Stab. 91 (2006) 769–777. https://doi.org/10.1016/j.polymdegradstab.2005.06.004.

[22] F. Carrasco, D. Dionisi, A. Martinelli, M. Majone, Thermal stability of polyhydroxyalkanoates, J. Appl. Polym. Sci. 100 (2006) 2111–2121. https://doi.org/10.1002/app.23586.

[23] M.C. Righetti, M.L. Di Lorenzo, Melting temperature evolution of non-reorganized crystals. Poly(3-hydroxybutyrate), Thermochim. Acta. 512 (2011) 59–66. https://doi.org/10.1016/j.tca.2010.08.023.

[24] L.M.W.K. Gunaratne, R.A. Shanks, Multiple melting behaviour of poly(3-hydroxybutyrate-co-hydroxyvalerate) using step-scan DSC, Eur. Polym. J. 41 (2005) 2980–2988. https://doi.org/10.1016/J.EURPOLYMJ.2005.06.015.

[25] N. Yoshie, H. Menju, H. Sato, Y. Inoue, Complex composition distribution of poly(3-hydroxybutyrate-co-3-hydroxyvalerate), Macromolecules. 28 (1995) 6516–6521. https://doi.org/10.1021/ma00123a018.

[26] M. Yasuniwa, T. Satou, Multiple melting behavior of poly(butylene succinate). I. Thermal analysis of melt-crystallized samples, J. Polym. Sci. Part B Polym. Phys. 40 (2002) 2411–2420. https://doi.org/10.1002/polb.10298.

[27] W.-T. Chuang, P.-D. Hong, H.H. Chuah, Effects of crystallization behavior on morphological change in poly(trimethylene terephthalate) spherulites, Polymer (Guildf). 45 (2004) 2413–2425. https://doi.org/10.1016/J.POLYMER.2004.01.048.

[28] P. Da Hong, W.T. Chung, C.F. Hsu, Crystallization kinetics and morphology of poly(trimethylene terephthalate), Polymer (Guildf). 43 (2002) 3335–3343. https://doi.org/10.1016/S0032-3861(02)00163-5.

[29] H.H. Chuah, Intrinsic birefringence of poly(trimethylene terephthalate), J. Polym. Sci. Part B Polym. Phys. 40 (2002) 1513–1520. https://doi.org/10.1002/polb.10211.

[30] B. Laycock, M. V. Arcos-Hernandez, A. Langford, S. Pratt, A. Werker, P.J. Halley, P.A. Lant, Crystallisation and fractionation of selected polyhydroxyalkanoates produced from mixed cultures, N. Biotechnol. 31 (2014) 345–356. https://doi.org/10.1016/j.nbt.2013.05.005.

[31] H. Wang, X. Zhou, Q. Liu, G.-Q. Chen, Biosynthesis of polyhydroxyalkanoate homopolymers by Pseudomonas putida, Appl. Microbiol. Biotechnol. 89 (2011) 1497–1507. https://doi.org/10.1007/s00253-010-2964-x.

[32] M. Saito, Y. Inoue, N. Yoshie, Cocrystallization and phase segregation of blends of poly(3-hydroxybutyrate) and poly(3-hydroxybutyrate-co-3-hydroxyvalerate), Polymer (Guildf). 42 (2001) 5573–5580. https://doi.org/10.1016/S0032-3861(01)00011-8.

[33] M.L. Cheng, Y.M. Sun, H. Chen, Y.C. Jean, Change of structure and free volume properties of semi-crystalline poly(3-hydroxybutyrate-co-3-hydroxyvalerate) during thermal treatments by positron annihilation lifetime, Polymer (Guildf). 50 (2009) 1957–1964. https://doi.org/10.1016/j.polymer.2009.02.025.

[34] J.A.S. Puente, A. Esposito, F. Chivrac, E. Dargent, Effect of boron nitride as a nucleating agent on the crystallization of bacterial poly(3-hydroxybutyrate), J. Appl. Polym. Sci. 128 (2013) 2586–2594. https://doi.org/10.1002/app.38182.

[35] G. Ivanova, L.S. Serafim, P.C. Lemos, A.M. Ramos, M.A.M. Reis, E.J. Cabrita, Influence of feeding strategies of mixed microbial cultures on the chemical composition and microstructure of copolyesters P(3HB-co-3HV) analyzed by NMR and statistical analysis, Magn. Reson. Chem. 47 (2009) 497–504. https://doi.org/10.1002/mrc.2423.

[36] Y. Doi, M. Kunioka, Y. Nakamura, K. Soga, Nuclear Magnetic Resonance Studies on Poly(β-hydroxybutyrate) and a Copolyester of β-Hydroxybutyrate and β-Hydroxyvalerate Isolated from Alcaligenes eutrophus H16, Macromolecules. 19 (1986) 2860–2864. https://doi.org/10.1021/ma00165a033.

# Processing window of Poly[R-3-hydroxybutyrate-co-(R-3-hydroxyvalerate)] (PHBV)

## New thermo-regulated WAXS experiments

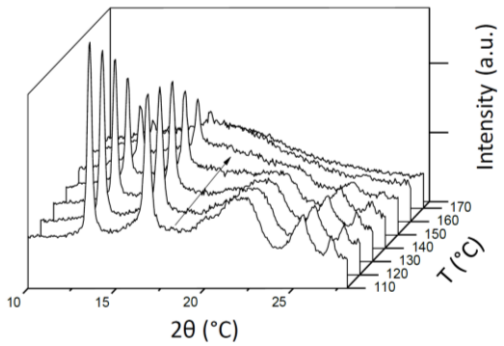


Definition of the minimal T°C to achieve complete melting

**Coupled to TGA and DSC**

Definition of the range of processing T°C to be tested

## Impact of T°C on crystallization and mechanical properties

### *(a) Too high processing T°C*

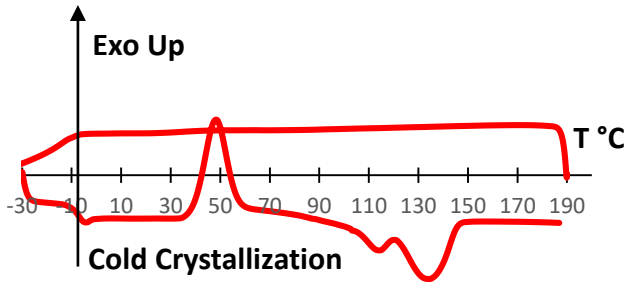


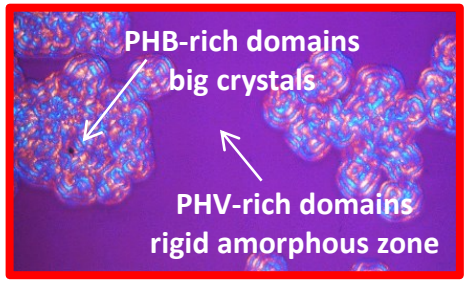


**Poor mechanical properties**

### *(b) Correct processing T°C*

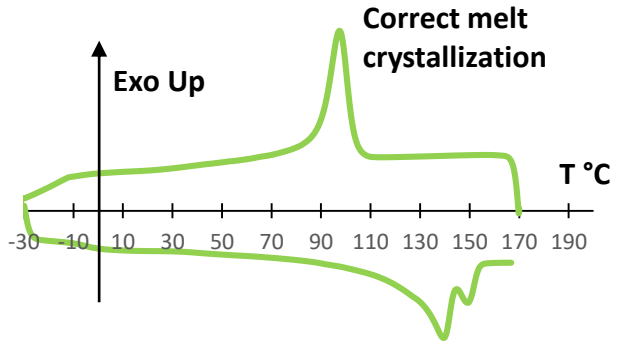


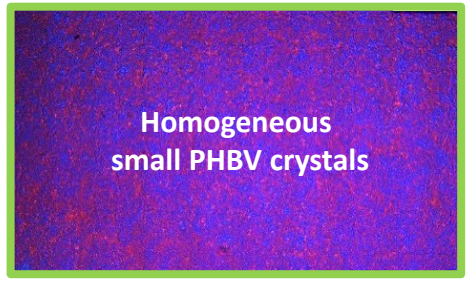


**Improved flexibility**

## Key messages

PHBVs are thermally-sensitive biopolymers

It is necessary to define the adequate processing windows to avoid degrading their final performance

A specific processing window can be found for each PHBV material